2024 IEEE/RSJ International Conference on Intelligent Robots and Systems (IROS)
October 14-18, 2024. Abu Dhabi, UAE

# A Wearable Mechanical Pressure-Electrophysiological Bimodal Sensing System for Rehabilitation Electromechanical Device

Peng Wang, Jixiao Liu, *Member, IEEE*, Dianpeng Qi, and Shijie Guo, *Member, IEEE*

***Abstract*—With the aging of society, there has been an increase in the number of elderly individuals with limb movement disorders. Active rehabilitation training using limb rehabilitation electromechanical devices that incorporate multimodal sensing and monitoring functions can significantly contribute to the recovery of limb motor functions. This report introduces a wearable mechanical pressure-electrophysiological monitoring bimodal sensing system specifically designed for human limb rehabilitation devices. By utilizing just four electrodes (SE, CE/DE, GND, REF), this system enables simultaneous and co-located measurement of surface electromyographic (sEMG), pressure, and mechanomyography (MMG) signals. These signals can be utilized to analyze muscle tension, stiffness, and tremor information. At last, this sensing system was used to assess muscle contraction force and localized muscle fatigue. The time and frequency domain characteristics of physiological signals during exercise were thoroughly investigated. The wearable mechanical pressure-electrophysiological bimodal sensing system can provide valuable data references for rehabilitation robots or human limb rehabilitation device, which is of great significance in the diagnosis of muscular diseases and rehabilitation treatment.**

## I. Introduction

Medical theory and clinical experience have demonstrated that early limb rehabilitation exercise training can effectively prevent muscular atrophy and aid in muscle functional recovery[1]. A portable and simple human limb rehabilitation electromechanical device with multimodal sensing monitoring plays a key role in exercise therapy, which can help patients or the elderly to engage in various scientifically-designed rehabilitation training programs[2].

The integration of myoelectric and mechanical signals during muscle contraction is essential in human-robot interactions[3-6]. To provide users with personalized services, a rehabilitation electromechanical system is developed based on the monitoring of human muscle state, which enables the creation of tailored rehabilitation training programs. Such systems often require a set of sensing system to detect human physiological information, facilitating the evaluation of muscle contraction and relaxation, local muscle fatigue, muscle endurance, and other related factors[7].

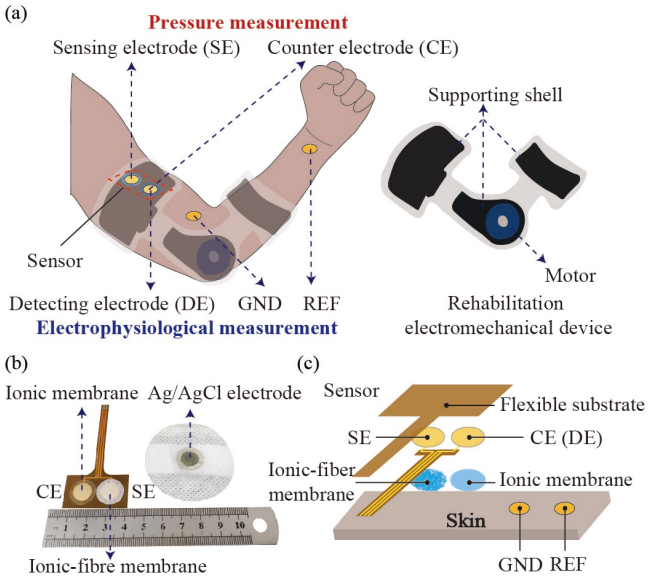


Figure 1. Wearable bimodal sensor pictures and functions. (a) Picture of the sensor attached to skin and rehabilitation electromechanical device for pressure-electrophysiological measurement. (b) Dimensions of the sensor. (c) Exploded view of the bimodal sensor.

Currently, the most commonly used method for evaluating muscle state in rehabilitation robots is through the measurement of surface electromyographic (sEMG) signals. sEMG signals represent the bioelectric currents generated by muscles on the surface of the human body during muscle contractions[8-9]. While the original sEMG signal allows for the observation and estimation of muscle strength and fatigue to some extent, it can only qualitatively analyze muscle strength and cannot directly provide muscle force feedback effects[10]. Therefore, there is a need for a wearable, compact, and highly integrated multifunctional sensor capable of simultaneously monitoring mechanical pressure and electrophysiological signals at the same location, providing a comprehensive expression of muscle status and function.

However, combining mechanical pressure sensors with electrophysiological sensors remains a significant challenge[11]. Until now, the integration of multimodal sensors measuring mechanical pressure and physiological electrical signals has primarily relied on the traditional approach of incorporating various sensing elements into a single system. Unfortunately, sensors produced through this traditional method typically require multiple materials to

Peng Wang is with the school of Mechanical Engineering, Hebei University of Technology, China and Hebei Key Laboratory of Smart Sensing and Human-Robot Interaction, Hebei University of Technology, Tianjin 300132 (e-mail: 202111201023@stu.hebut.edu.cn).

Jixiao Liu is with the school of Mechanical Engineering, Hebei University of Technology, China and Hebei Key Laboratory of Smart Sensing and Human-Robot Interaction, Hebei University of Technology, Tianjin 300132 (corresponding author, phone: 86-185-2209-9429; e-mail: liujixiao@hebut.edu.cn).

Dianpeng Qi is with School of Chemical Engineering, Harbin Institute of Technology, Harbin 150006.

Shijie Guo is with the school of Mechanical Engineering, Hebei University of Technology, China and Hebei Key Laboratory of Smart Sensing and Human-Robot Interaction, Hebei University of Technology, Tianjin 300132.

heterogeneously integrate different components, resulting in several drawbacks such as complex manufacturing processes, limited portability, unsuitability for wearing, and difficulties in data measurement correspondence.

In this study, we present a flexible, combinatorial structure, and low-energy wearable bimodal sensing system designed specifically for rehabilitation robots or human limb rehabilitation devices to monitor muscle rehabilitation status. Utilizing just four electrodes (SE, CE/DE, GND, REF), this system enables simultaneous and co-located measurement of sEMG, pressure, and even mechanomyography (MMG) signals. MMG is a mechanical signal that records lateral vibrations during muscle contraction. Compared to sEMG, it is less affected by electrical interference, making it suitable for various environments and conditions.

## II. The Bimodal Sensing System

We have built a bimodal sensing system that includes a wearable bimodal flexible sensor, sensor circuit module, and host computer. In this section, the structure, principle and sensing characteristics of the bimodal sensor are described.

### *A. The Structure of The Bimodal Sensor*

In this work, the electrodes of the sensor including pressure sensing electrode (SE), counter electrode/detection electrode (CE/DE, one shared electrode). The sensor containing SE and CE/DE is attached to the skin with a medical tape. In addition, two commercial electrodes are attached to the skin in the correct position, the grounding electrode (GND) and the reference electrode (REF). SE and CE are utilized for pressure measurement, while DE, REF, and GND are employed to measure electrophysiological signals, as shown in Figure 1(a). Due to the use of the shared electrode (CE/DE), the total number of electrodes is 4, which is less than the traditional integrated bimodal sensing system[12]. The rehabilitation electromechanical device is used to control the movement of the body's joints and to provide support shell for sensors.

Based on our previous research[13] on tactile sensor, we chose ionic-fibre membrane as the sensing material for SE and ionic membrane ([EMIM]NTf2:PVDF-HFP = 1:1) as the material for shared electrode CE, as shown in Figure 1(b). The two electrodes of the sensor form a pathway through the skin in the form of a skin-electrode, with one electrode providing a solid electrolyte material with a microstructure as SE, and the other electrode providing a solid electrolyte material in conformal contact with the skin as CE. In addition, due to the low impedance of the solid ionic electrolyte under high frequency[14], the material of CE is also suitable for electrophysiological electrodes.

The exploded view of the sensor structure is shown in Figure 1(c). We use FPC as the flexible substrate of the sensing material, and the dimensions of both SE and CE are circular with a diameter of 10 mm, and the distance between the centers of the two electrodes is 15 mm. The electrode surfaces are gold-plated without insulation, and the remaining leads are insulated. The ionic fibre membrane and the ionic membrane are circular in size with a diameter of 15 mm and are attached to the SE and CE, respectively. Finally, the sensor patch was attached to the skin using medical tape, and the REF and GND electrodes were attached at the corresponding locations on the skin, and the leads were introduced into the signal acquisition circuit board for pressure-electrophysiological measurements.

### *B. Sensing Principle*

Sensing schematic of the bimodal sensor as shown in Figure 2(a). When SE is not subjected to external pressure, the contact area of the ionic fibre membrane with the electrode and the skin is small, and most of the ions remain free in the ionic fibre membrane. The capacitance value of the sensor is small at this time. However, when the SE electrode of the sensor is subjected to external compressive force, the contact area of the ionic fibre membrane with the electrode and the skin interface increases after compression. At this point, the anions and cations in the ionic-fibre membrane towards the electrode with opposite charge under the attraction of the SE positive and negative electrons and the anions and cations in the skin. Since the ions are unable to exchange charges with electrons across the interface, a double electric layer is formed at the interface, and the capacitance increases as the interfacial contact area increases. When CE is subjected to an external compressive force, the capacitance remains stable due to the conformal contact interface of the ionic membrane. CE/DE is used as a qualified electrode for the detection of electrophysiological signals, which is insensitive to pressure signals, and forms a three-electrode system for the measurement of electrophysiological signals together with GND and REF.

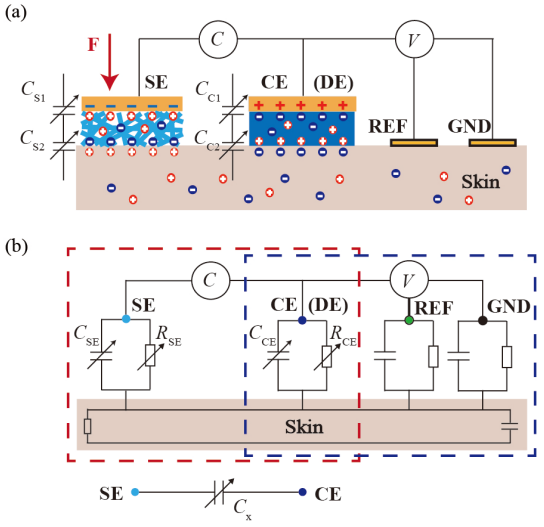


Figure 2. Sensing principle of the bimodal sensor. (a) Sensing schematic of the bimodal sensor. (b) Equivalent circuit diagram of the bimodal sensor.

Equivalent circuit diagram of the bimodal sensor as shown in Figure 2(b). SE and CE form double electric layers with skin, respectively. $C_{S1}$, $C_{S2}$ represent the capacitance of the SE/solid electrolyte interface (variable contact area) and solid electrolyte/skin interface (variable contact area), respectively. They are equal in value and can be equivalent to $C_{SE}$. Similarly, $C_{C1}$, $C_{C2}$ are equivalent to $C_{CE}$, with conformal contact interfaces at the CE. $C_{SE}$ is related to the

variation of the two contact areas at SE, while $C_{CE}$ remains constant. $C_{CE}$ has the same value with $C_{SE}$ because the charge at the interfaces of CE and SE follow the law of charge conservation. $R_i$ represents the resistance between the two electrodes; $C_E$ represents the coupling capacitance of the parallel electrodes, which is small and can be negligible. According to the simplified equivalent circuit diagram of pressure sensing in Figure 2(b), the capacitance $C_x$ between the two electrodes roughly follows $1/C_x = 1/C_{SE} + 1/C_{CE}$. Since $C_{CE}$ varies with $C_{SE}$, the signal output is determined by the capacitance $C_{SE}$, which is a function of the applied pressure.

### C. Sensing Characteristics

A digital manometer equipped with a 10 mm diameter probe is utilized to exert pressure upon the SE. We used an LCR meter to measure the capacitance between the two electrodes to characterise the pressure applied to the sensor. The LCR meter was set by default to 30 kHz and 1.65 V for testing in the measurements. Physiological electrical signals were acquired using the High-Performance and High-density Acquisition System of Neuromuscular Electrophysiological Signals, model NES-16B01.

Based on the above analyses of the structure and principle of pressure sensing, we attached the sensor to the skin of the forearm and pressed the two electrodes separately with a glass rod. As shown in Figure 3(a), the measured capacitance value increased sharply when SE was pressed, while the measured capacitance value remained basically unchanged when CE was pressed.

The characteristic curve between applied pressure and sensor capacitance is shown in Figure 3(b). The pressure range of the sensor can reach 0~320 kPa, and the pressure range of the pressure measurement strategy in this paper is widened by more than 20 times compared with that of the similar parallel skin electrode structure [15] (about 0~15 kPa). The sensitivity of a capacitive pressure sensor is usually defined as $S = \delta(\Delta C/C_0)/\delta P$, where $C_0$ is the capacitance before loading, $\Delta C$ is the change in capacitance, and $P$ is the applied pressure. We find that the sensor exhibits a good linear response, with a sensitivity $S$ of 0.41942 $kPa^{-1}$ over the pressure range of 0 to 320 kPa, and the sensor has a high degree of linearity (R-Squared of 0.99023), so we can obtain the calibrated equation of the relationship between capacitance $C$ and pressure $P$, $\Delta C/C_0 = S*P + C_0$. We tested the sensor's limit of detection (LOD) by placing weights (1 g, 2 g, 5 g, 10 g) on the SE, resulting in an LOD of 24.8 Pa.

The sEMG signal acquired by the sensor is shown in Figure 3(c), it can be seen that the sEMG signals measured by the sensor and Ag/AgCl commercial electrode were basically the same at grip forces of 20 LB, 40 LB, and 60 LB. The signal to noise ratio (SNR) of the sEMG signals of DE electrode and Ag/AgCl commercial electrode were 30.36 dB and 29.67 dB when holding a 60 LB grip circle, respectively. The result indicate that the electrophysiological signals measured by the DE are of comparable quality to those obtained from Ag/AgCl commercial electrodes. The motion artifacts of the electromyographic signal are shown in Figure 3(d). Due to the impedance changes at the electrode skin contact interface, motion artifacts are generated. However, compared to commercial electrodes, the motion artifacts generated by the sensor DE are smaller.

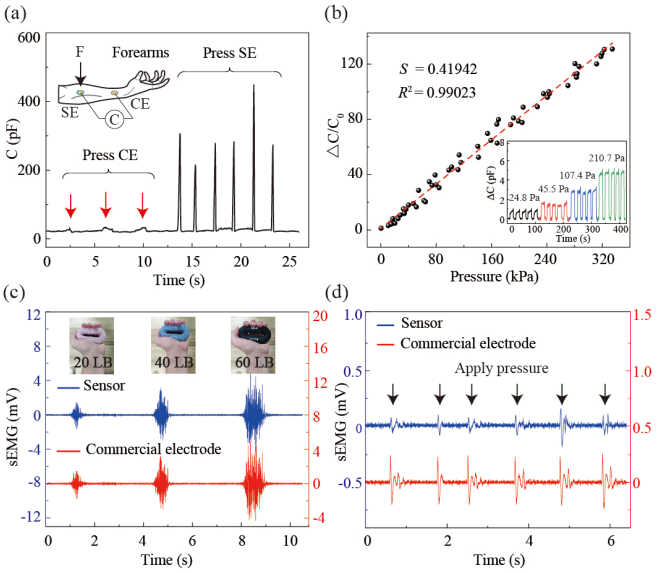


Figure 3. Characterization of mechanical pressure signals and electrophysiological signals of the bimodal sensor. (a) Sensor response when touching SE and CE with a glass rod. (b) Characteristic curve between the pressure applied to the SE and the differential capacitance. (c) The sEMG signal acquired by the sensor is essentially the same as that of commercial electrodes. (d) Effect of applied pressure on sensor electrophysiological signal.

## III. Data Acquisition and Processing

### A. Sensor Circuit Module

The schematic diagram of pressure and electrophysiological signal acquisition is shown in Figure 4. In the pressure measurement circuit, the sensor is connected in series with the sampling capacitor ($C_s$) to form a voltage divider circuit. By simplifying the multiple solid electrolyte layers between SE and CE to a single solid electrolyte layer, the sensor can be roughly equated to a variable capacitance $C_x$. $V_0$ is the sinusoidal source voltage, and $V_x$ is the voltage at both ends of $C_s$, which varies with $C_x$ and has a functional relationship with pressure. The $V_x$ were sampled at a frequency of 100 Hz. The electrophysiological signal measurement circuit collects electrophysiological signals $V_E$ through an ADS1298 analog-to-digital converter and the sampling frequency is 1000 Hz..

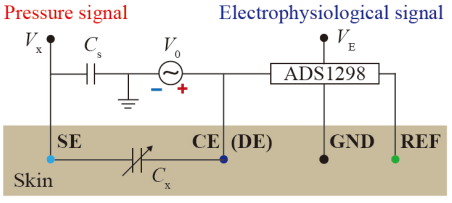


Figure 4. Bimodal sensor module circuit principle for pressure measurement and electrophysiological measurement.

### B. *Pressure Calibration*

The capacitive resistance of the capacitor can be expressed as:

$$X = \frac{1}{2\pi f C} \tag{1}$$

Where $f$ is the frequency of the sinusoidal signal source; $C$ is the capacitance value.

The equivalent circuit of the sensor pressure module circuit is shown on the left side of Figure 4, and $V_x$ can be expressed as:

$$\frac{V_x}{V_0} = \frac{X_s}{X_s + X_c} \tag{2}$$

The inferred value of $C_x$ can be obtained from (1) and (2):

$$C_x = \frac{C_s V_x}{V_0 - V_x} \tag{3}$$

Where $V_0$ is the amplitude of the sinusoidal signal source voltage. In this study, $V_0$ is 1.65 V.

In addition, according to Figure 3(b), the relationship between $C_x$ and $P$ can be fitted as follows:

$$C_x = S * C_0 * P + C_0 \tag{4}$$

The formula for the relationship between $P$ and the circuit acquisition voltage $V_x$ can be obtained from (3) and (4):

$$P = \frac{1}{SC_0} * \left( \frac{C_s V_x}{V_0 - V_x} - C_0 \right) \tag{5}$$

Where $S$ is the sensitivity of the sensor; $C_0$ is the initial capacitance of the sensor attached to the skin.

### C. *Data Processing*

The raw data were processed as shown in Figure 5, the pressure signal is obtained by low-pass filtering of the raw pressure data at 2 Hz, while the MMG signal is obtained by high-pass filtering of the raw pressure data at 2 Hz. The raw sEMG data were is firstly high-pass filtered at 10 Hz using a fourth-order Butterworth filter, then the narrow bandwidth interference in the recorded signal is eliminated by linear recursive digital notch filter, and finally the noise signal in the electrophysiological signal is removed by Daubechies 5 (DB5) wavelet noise reduction.

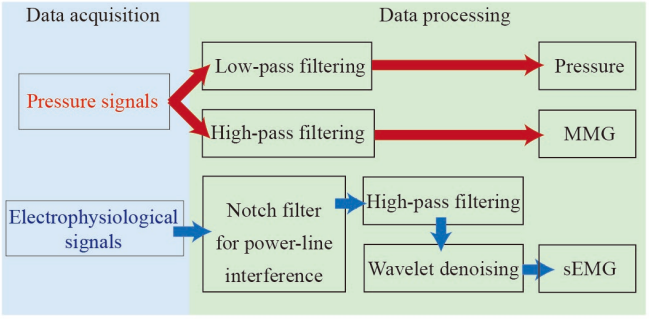


Figure 5. Data processing methods for pressure, MMG, and sEMG.

## IV. Muscle Condition Monitoring Applications

The application of the bimodal sensing system combined with rehabilitation electromechanical device is shown in Figure 6. In this section, we tested the effectiveness of the bimodal sensing system for the evaluation of muscle contraction force and muscle fatigue.

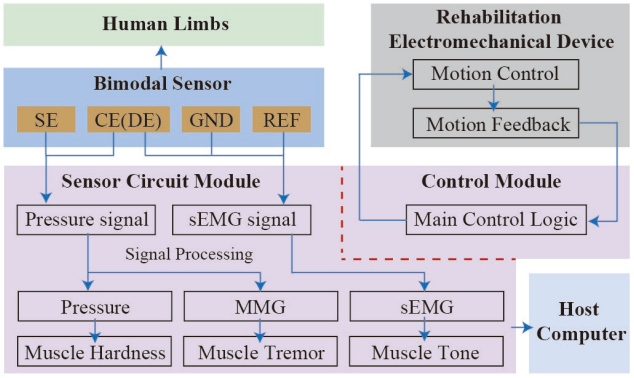


Figure 6. The application of the bimodal sensing system for rehabilitation electromechanical device.

### A. *Muscle Contractility Evaluation*

It has been demonstrated that under non-fatiguing activity conditions, the contractility of the locomotor muscles is proportional to the changes in several indices of sEMG, such as integrated EMG (iEMG), root mean square (RMS), median power frequency (MPF), and median frequency (MF), within a certain muscle maximal voluntary contraction (MVC) range.

In order to investigate the role of the wearable bimodal sensor system in evaluating muscle contraction function, this paper focuses on the test of biceps brachii muscle. The bimodal sensor synchronously collects mechanical pressure and electrophysiological signals during the isometric exercise using 1 kg, 2 kg, and 5 kg dumbbells for 10 repetitions. The signals are analyzed in the time and frequency domains to provide quantitative data as a reference for movement disorders in elderly people.

The measurement and calculation results are shown in Figure 7, we find that the muscle shows periodic changes in sEMG and pressure signals during isotonic movement. Under the same load, we can see the changes of sEMG and pressure signal during the exercise cycle. When the arm reaches the highest point, the muscle contraction force and muscle hardness are the largest, at which time the pressure signal and EMG signal amplitude are the highest; when the arm is at the lowest point, the muscle contraction force and muscle hardness are the smallest, at which time the pressure signal and EMG signal amplitude are the lowest. In addition, the indices of the sEMG showed similar trends during the exercise cycle.

Under different loads, muscle tone, muscle stiffness and muscle tremor increased with increasing load, so the amplitudes of muscle sEMG, pressure signal and MMG were proportional to the arm load.

In addition, pressure signals can to some extent express muscle hardness, and the rate of pressure change represents the speed of muscle response. The greater the load on the arm, the harder the muscles need to reach in a short period of time, so the speed of pressure change is also proportional to the load on the arm.

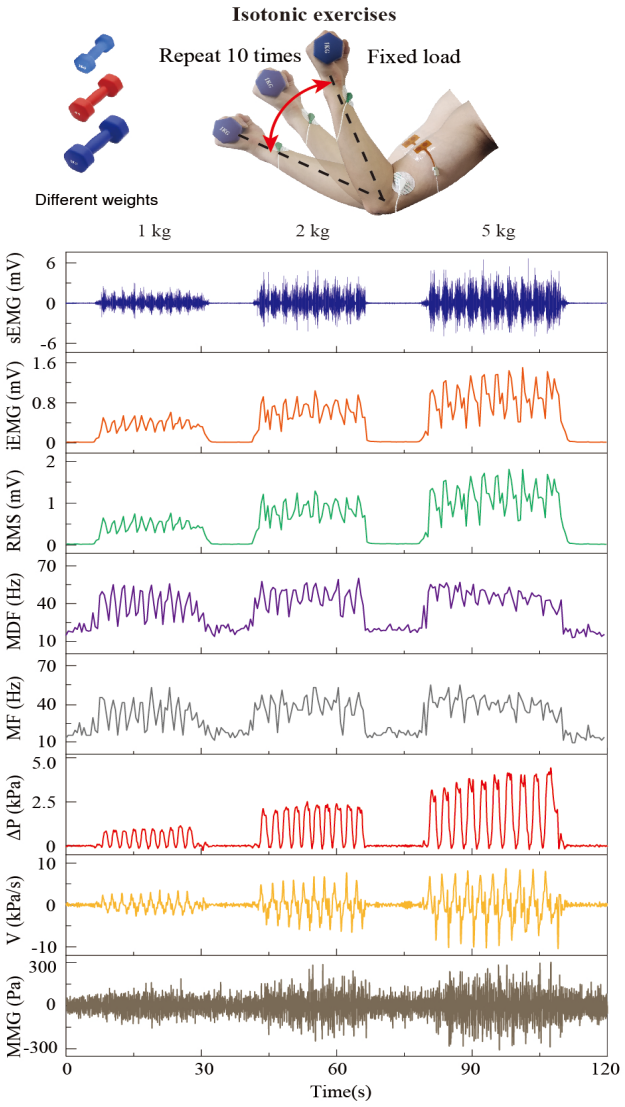


Figure 7. The sEMG, pressure, MMG and eigenvalue changes in time and frequency domains during isotonic exercise of the biceps brachii muscle.

## B. *Muscle Fatigue Monitoring*

The electromyographic and mechanical signals of muscles are two important references in the evaluation of localized muscle fatigue, and the quantitative analysis of electromyographic and pressure signals can be used to develop appropriate planning for muscle training and thus to improve muscle athletic ability or rehabilitation. We utilized a bimodal sensing system to measure the pressure-sEMG signals of the biceps brachii muscle during isotonic movements that persisted to the point where the posture could not be maintained to assess muscle fatigue.

The measurement and calculation results are shown in Figure 8, we recorded sEMG signals, pressure signals, and MMG signals during biceps exercise for approximately 100 s. We analyze the time-domain and frequency-domain characteristics of the sEMG and MMG signals with a period of 10 s. As muscle fatigue increased, RMS showed an increasing trend and MPF showed a decreasing trend.

Since fatigued muscles need to activate more muscle fibers to maintain the required force, the RMS amplitude of the sEMG signal is significantly higher in fatigued muscles than in non-fatigued muscles. In addition, fast-twitch muscle fibers fatigue more quickly than slow-twitch fibers, leading to in a decrease in MPF.

As muscle fatigue increases, muscle tremor leads to an increase in RMS of the MMG signal. Additionally, the RMS value of the MMG signal increases dramatically between 110 and 120 seconds, representing a significant rise in muscle tremor, which prevents maintaining the movement.

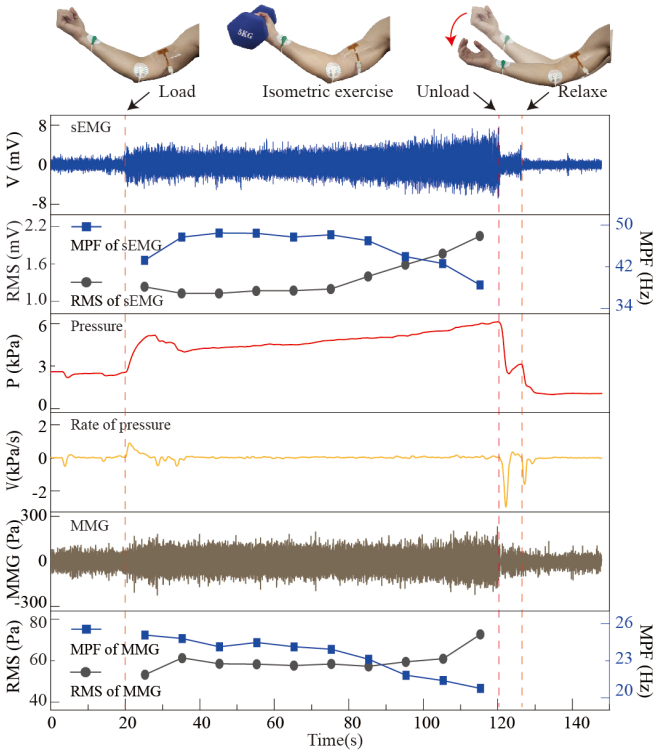


Figure 8. Electrophysiological and pressure signals measured by the bimodal sensing system during fatigue testing of the biceps brachii under isometric and constant force (5 kg) contraction.

## V. Conclusion

In this research, we present a wearable bimodal sensing system that combines mechanical pressure and electrophysiological measurements, specifically designed for rehabilitation electromechanical devices. We provide an overview of the sensor's structure, sensing principle, and characteristics, along with the data acquisition and processing methods employed in the circuit module. Furthermore, we conducted tests to evaluate muscle

contraction force and muscle fatigue using this sensing system. The results demonstrate that our sensing system has the capability to assess muscle tone, hardness, and tremor by analyzing signals from sEMG, pressure, and MMG. This sensing system plays an important role in diagnosing muscle diseases such as muscle atrophy, muscle rigidity, and muscle rehabilitation training by detecting various muscle parameters. It offers valuable physiological information about human limb muscles, enabling rehabilitation robots or electromechanical devices to diagnose muscle disorders and develop personalized rehabilitation training programs. The findings of this study hold significant implications in the field of exercise therapy.

## REFERENCES


[1] Forbrigger Shane, DePaul Vincent G, Davies T. Claire, Morin Evelyn, Hashtrudi-Zaad Keyvan. "Home-based upper limb stroke rehabilitation mechatronics: Challenges and opportunities," *BioMedical Engineering Online*, vol. 22, no. 1, p. 67, 2023.

[2] R.A.R.C. Gopura, D.S.V. Bandara, Kazuo Kiguchi, G.K.I. Mann. "Developments in hardware systems of active upper-limb exoskeleton robots: A review," *Robotics and Autonomous Systems*, vol. 75, pp. 203-220, 2016.

[3] Kyrkjebo Erik, Laastad Mads Johan, Stavdahl Oyvind, "Feasibility of the UR5 industrial robot for robotic rehabilitation of the upper limbs after stroke," in *2018 IEEE/RSJ International Conference on Intelligent Robots and Systems (IROS)*, IEEE 2018, pp. 6124-6129.

[4] Ogata Kunihiro, Hirabayashi Yuto, Kubota Keisuke, Tsuji Toshiaki, "Home rehabilitation assist robot to facilitate isolated movements for hemiplegia patients", in *2017 IEEE/RSJ International Conference on Intelligent Robots and Systems (IROS)*, IEEE 2017, pp. 527-532.

[5] Antonella Belfatto, Alessandro Scano, Andrea Chiavenna, Alfonso Mastropietro, Simona Mrakic-Sposta, Simone Pittaccio, Lorenzo Molinari Tosatti, Franco Molteni, Giovanna Rizzo. "A multiparameter approach to evaluate post-stroke patients: An application on robotic rehabilitation," *Applied Sciences*, vol. 8, no. 11, p. 2248, 2018.

[6] Ceglia Amedeo, Bailly Francois, Begon Mickael. "Moving horizon estimation of human kinematics and muscle forces," *IEEE Robotics and Automation Letters*, vol. 8, no. 8, pp. 5212-5219, 2023.

[7] Jeoung Bogja, Choi Muncheong, Kim Alchan. "Development and performance evaluation of a smart upper-limb rehabilitation exercise device," *Sensors*, vol. 24, no. 2, p. 659, 2024.

[8] Sedighi Paniz, Li Xingyu, Tavakoli Mahdi. "EMG-based intention detection using deep learning for shared control in upper-limb assistive exoskeletons," *IEEE Robotics and Automation Letters*, vol. 9, no. 1, pp. 41-48, 2024.

[9] Kazuo Kiguchi, Yoshiaki Hayashi. "An EMG-based control for an upper-limb power-assist exoskeleton robot." *IEEE Transactions on Systems, Man, and Cybernetics, Part B: Cybernetics*, vol. 42, no. 4, pp. 1064-1071, 2012.

[10] Khan Salman Mohd, Khan Abid Ali, Farooq Omar. "Selection of features and classifiers for EMG-EEG-based upper limb assistive devices-A review," *IEEE Reviews in Biomedical Engineering*, vol. 3, pp. 248-260, 2020.

[11] Desplenter Tyler, Zhou Yue, Edmonds Brandon Pr, Lidka Myles, Goldman Allison, Trejos Ana Luisa. "Rehabilitative and assistive wearable mechatronic upper-limb devices: A review," *Journal of Rehabilitation and Assistive Technologies Engineering*, vol. 7, p. 205566832091787O, 2020.

[12] Chun Kyoung-Yong, Seo Seunghwan, Han Chang-Soo. "A wearable all-gel multimodal cutaneous sensor enabling simultaneous single-site monitoring of cardiac-related biophysical signals," *Advanced Materials*, vol. 34, no. 16, p. 2110082, 2022.

[13] Jixiao Liu, Manfei Wang, Peng Wang, Funing Hou, Chuizhou Meng, Kazunobu Hashimoto, Shijie Guo. "Cost-Efficient Flexible Supercapacitive Tactile Sensor With Superior Sensitivity and High Spatial Resolution for Human-Robot Interaction," *IEEE Access*, vol. 8, pp. 64836-64845, 2020.

[14] Kim Yong Min, Moon Hong Chul. "Ionoskins: Nonvolatile, highly transparent, ultrastretchable ionic sensory platforms for wearable electronics," *Advanced Functional Materials*, vol. 30, no. 4, p. 1907290, 2020.

[15] Zhu Pang, Du Huifeng, Hou Xingyu, Lu Peng, Wang Liu, Huang Jun, Bai Ningning, Wu Zhigang, Fang Nicholas X, Guo Chuan Fei. "Skin-electrode iontronic interface for mechanosensing," *Nature Communications*, vol. 12, no. 1, p. 4731, 2021.